Super-Bainite

Francisca G. Caballero and Carlos Garcia-Mateo

Department of Physical Metallurgy, National Center for Metallurgical Research (CENIM-CSIC), Avda Gregorio del Amo, 8; Madrid, E-28040, Spain.
fgc@cenim.csic.es; c.g.mateo@csic.es

Abstract:

In this work, the history of recent developments related to the so-called Super-Bainite or nanocrystalline bainite is reviewed. This microstructure has aroused the interest of the scientific and technological community, due to the intricate and complex characteristics that define its structure, as well as the excellent mechanical properties. It has been needed fundamental studies at the atomic scale to establish the most relevant property-microstructure relationships. This work offers a guided journey to understand Super-bainite, from the atomic level to full size components.

Keywords: Steel, Nanocrystalline Steel, Solid Reaction, Displacive Transformation, Bainite, Carbon Supersaturation, Tetragonal Ferrite, Carbon Clustering, TRIP Effect, TWIP Effect

Super-Bainite: a nanocrystalline steel formed by solid reaction

By definition, in a nanocrystalline metal at least one internal length scale should be smaller than 100 nm (Whang 2011). They contain an exceptionally large density of strong interfaces, rather than only a minor fraction of features such as precipitates, which are small in size. Thermomechanical processes, heat treatments or alloying additions are the traditional strategies to produce ultra-fine grained metals (100 nm–1 μm) (Humphreys, Prangnell et al. 2001), whereas deposition-based processes and severe plastic deformation processes ensure the nanocrystallization (<100 nm) of metal structures (Erb, Palumbo et al. 2011, Valiev 2011).

In steels, displacive transformations can be exploited in order to obtain heavily refine ferritic crystals at low temperatures or by rapid cooling (Krauss 2005). Ultra-fine needle-shaped ferrite crystallites as in martensite and bainite grow by displacive transformation (Bhadeshia and Honeycombe 2006). These solid reactions involve a sudden, ordered movement of iron atoms, which is accompanied by a given crystal correspondence, and a macroscopic shape strain of the transformed structure (Christian, Olson et al. 1995) (Swallow and Bhadeshia 1996). The transformation products are restricted to the prior austenite grain and exhibit a characteristic hierarchy sub-structure of aggregates of very thin ferrite plates (Christian 1958, Morito, Huang et al. 2006, Takayama, Miyamoto et al. 2012).

In bainite reaction, the shape change is partially accommodated plastically, and the introduced defects limit the final size of formed plates, becoming thinner at low temperature when the austenite is harder (Chang and Bhadeshia 1995). Following this simple concept, modern steels, known as Super-Bainite (Caballero and Bhadeshia 2004), have been designed with the solely purpose of achieving low transformation temperatures (125-325 ° C) that ultimately result in a nanoscale microstructure. A mixture of extremely fine bainitic ferrite plates, 20–40 nm thick, interwoven with even thinner films of retained austenite, are the hallmarks of these microstructures (Caballero, Garcia-Mateo et al. 2014), that are obtained in high carbon (0.6–1.0% by weight) high silicon (1.5–3.0% by weight) steels by simple isothermal heat treatments above their martensite start, Ms, temperatures (~120 ° C). The driving force for the development and upscaling of super-bainitic steels (detailed compositions are given in Table 1) has undoubtedly been the unrivaled combination of strength and ductility (UTS up to 2075 MPa with a total elongation of 20%), an outstanding wear performance, and competitive values for fatigue strength (Caballero and Bhadeshia 2004, Garcia-Mateo, Caballero et al. 2012, Sourmail, Caballero et al. 2013, Caballero, Garcia-Mateo et al. 2014).

<Table 1 near hear>

The first generation of super-bainitic steels exhibited very slow transformation kinetics during bainite reaction (Caballero, Garcia-Mateo et al. 2014), i.e. in the case of the two first developed steels (Super-Bainite 0 and 1), the transformation needed from 2 to 90 days to complete in the temperature range 125–325ºC. With an eye on future commercialization, the need to shorten transformation times was imperative. So, in a second development within the first generation of Super-Bainite, the addition of controlled additions of cobalt and aluminum (Super-Bainite 2 and 3 steels) boosted the driving force for transformation causing a significant drop of the time to complete the process, coming down to hours as opposed to days (Garcia-Mateo, Caballero et al. 2003).

Additional research within the framework of a collaborative project, allowed to further increase the transformation rate by controlling the chemical composition, reducing the carbon, manganese, chromium and molybdenum contents and also by refining the austenite grain size with the help of niobium additions (Sourmail, Caballero et al. 2013), leading to the development of the second generation of Super-Bainite. As a result, Super-Bainite 4-12 steels were fully transformed in less than 10 hours for a temperature range of 220–350ºC (Caballero, Garcia-Mateo et al. 2014). However, their exploitation is still limited to niche applications, the main difficult arising from welding, as brittle martensite forms in the coarse grained heat affected zones of the joints (Fang, Yang et al. 2012), consequence of their high carbon content.

Therefore, the open question nowadays still remains in how to transfer the nano-scale bainite concept to lower carbon contents without deteriorating the superior combination

of the mechanical and technological properties (Garcia-Mateo, Paul et al. 2017). In this regards, and over the time, different approaches have been adopted. Yang and Bhadeshia (Yang and Bhadeshia 2008) introduced significant quantities of alloying elements, (2.3% Mn and 5% Ni wt. %) to solid solution strengthen the austenite while maintaining a low carbon content (0.1–0.2 wt. %). Austenite strength and dislocation density are the main factors controlling the refinement of bainitic microstructure by increasing the resistance to interface motion (Singh and Bhadeshia 1998, Cornide, Garcia-Mateo et al. 2013). Indeed, it was found that bainitic transformation temperatures can be suppressed, but unlike the high carbon steels, the difference between Bs and Ms decreases drastically at high solute concentrations (Yang and Bhadeshia 2008). Furthermore, it was found that the platelets of bainite tend to coalesce at low temperatures by an excess of available free energy during the transformation (Ohmori, Ohtsubo et al. 1994), which contradicts the initial objective.

Other researchers (Wang, Wu et al. 2014, Li, Huang et al. 2016) managed to obtain Super-Bainite in medium carbon steels by means of multistep heat treatments. The underlying concept of this approach is the continuous carbon enrichment of austenite due to partial bainitic transformation after each step. The treatment has proven effective in accelerating bainitic transformation and in refining the microstructure in the final stages of transformation (Zhao, Qian et al. 2016), but the great difficulty of being industrially implemented has also been proven.

However, a new approach is recently being explored in which bainitic transformation begins from a plastically deformed austenite, ausforming, (Gong, Tomota et al. 2010, Timokhina, Beladi et al. 2011, Gong, Tomota et al. 2013, Zhang, Wang et al. 2013, Zhang, Wang et al. 2014, Zhang, Wang et al. 2014, He, Zhao et al. 2015, He, Zhao et al. 2015). The advantages of this procedure could be summarized as follows. The increase in nucleation sites leads to an acceleration of the sluggish bainitic transformation. The consequent decrease in the Ms temperature due to plastic deformation, increases the temperature range for bainitic transformation (Bs-Ms) and brings it to even lower temperatures, and finally. Given that bainite starts from a plastically hardened austenite there is the possibility of a further refinement of the bainite lath size, therefore enhancing the hardness (Zhang, Wang et al. 2014, Garcia-Mateo, Paul et al. 2017).

From the crystallographic point of view, an advantage of this process, as compared with more conventional thermomechanical routes where deformation is applied at higher temperatures, is that the former can be employed to drastically reduce the number of bainite variants within a single austenite grain, leading to an extra refinement of the microstructure (Gong, Tomota et al. 2010, Gong, Tomota et al. 2013). Furthermore, the isotropy of the bainitic transformation can be altered by plastically deforming austenite prior to transformation, and the attained level of anisotropy will depend on the balance between the driving force of the transformation and the ability to promote certain crystallographic variants due to the variant selection induced by plastic deformation (Eres-Castellanos, Morales-Rivas et al. 2018).

It seems that in recent literature there is not a thorough study of the alloy design, process parameters, microstructure and mechanical response leading to obtain Super-Bainite in medium carbon ausformed steels (Garcia-Mateo, Paul et al. 2017). Such a study is the subject of *TIANOBAIN,* an ongoing European project entitled 'Towards industrial applicability of (medium carbon) nanostructured bainitic steels' (RFCS-2015-709607) that is expected to conclude with a recommendation of alloy chemical compositions and process parameters for industrial full-scale production of the third generation of Super-Bainite.

Multiscale Structural Analysis of Super-Bainite

The rationalization to the unprecedented mechanical performance of super-bainitic steels has only been possible after the comprehensive examination of the structure at several length scales. The multiscale characterization of these structures has revealed an intricate phase distribution and carbon accumulation at atomic scale.

<Figure 1 near here>

Figure 1 shows Super-Bainite at different magnifications. It is a composite-like structure of two phases, ferrite (α) and austenite (γ). Silicon addition in the steel avoids the precipitation of cementite from austenite during bainite reaction, stabilizing austenite in the structure (Bhadeshia 2015). Depending on the transformation temperature, a significant amount of austenite (25–50%) is retained in the ferritic matrix exhibiting a variety of shapes and sizes, as the SEM image in Figure 1a illustrates. Given their different locations in the structure, nano-scale films between ferrite plates are able to trap much more carbon than blocks by solute partitioning, which results in a complex carbon distribution in austenite essential to control the austenite stability (Caballero, Garcia-Mateo et al. 2009).

The high density of defects in Super-Bainite is apparent close to the austenite/ferrite interface in TEM images (Figure 1b). They are generated by plastic relaxation in austenite during the displacive reaction. Cornide et al. (Cornide, Miyamoto et al. 2011) determined the dislocation density in ferrite in super-bainitic steels by TEM to be (5.1 ± 2.7) x 10^{14} m^{-2}. This value is higher than those reported for conventional bainite, 1.7 x 10^{14} m^{-2} and, in general terms, similar to those measured for martensitic microstructures. In addition, multiple planar faults/twins in films of austenite are clearly observed, see Figure 1c (Bhadeshia and Edmonds 1979). Carbon might also segregate at these defects, therefore interfering in the carbon partitioning process into austenite after ferrite formation (Caballero, Yen et al. 2011).

Examination of Super-Bainite at high resolution has revealed remarkable analogies between Super-Bainite and martensite at an early stage of ageing. Figure 2 (a) shows a HR-TEM image of the ferritic phase of Super-Bainite transformed at 250ºC revealing local variation of the modulated structure in good agreement with previous observations in Fe−C martensite (Kusunoki and Nagakura 1981, Han, van Genderen et al. 2001). The satellite spots in the corresponding Fast Fourier Transform (FFT) in Figure 2b arise from the spatial periodicities associated with the broad fringes in the HR-TEM image. According to the present TEM observations, the overall structure consists of Fe atoms arranged according to a bct crystal lattice with carbon-enriched and carbon-depleted regions.

<Figure 2 near here>

In addition, there are significant evidences on the tetragonality of Super-Bainite based in extensive X-ray diffraction (XRD) analysis (Garcia-Mateo, Jimenez et al. 2015, Rementeria, Jimenez et al. 2017) and synchrotron radiation experiments (Hulme-Smith, Lonardelli et al. 2013, Rementeria, Jimenez et al. 2017). Table 2 lists results of Rietveld XRD analyses as reported elsewhere (Rementeria, Capdevila et al. 2018, De-Castro, Rementeria et al. 2020) on super-bainitic structures in comparison with martensite and tempered martensite.

<Table 2 near here>

It should be noted that tetragonality values reported in this table for bainite formed at low temperatures resembles those values for martensite tempered at similar temperature, but they are an order of magnitude lower than the tetragonality of fresh martensite in the same steel. The fact that regardless of the extended time after transformation at 220ºC in the 0.7 wt.% C steel, the c/a ratio and the carbon content in the ferrite remains nearly constant is a clear indicative that carbon supersaturated tetragonal ferrite is the metastable equilibrium crystal structure resulting from the transformation.

In order to rationalize the growth nature of bainitic ferrite, the best criterion determine if bainitic ferrite has the paraequilibrium (PE) carbon content or it is supersaturated in carbon. In the last decade, the use of modern analysis techniques to quantitative assess bainitic ferrite carbon content has become essential to explain bainite growth mechanisms (Pereloma 2016).

Figure 3 shows carbon distribution in bainitic ferrite as detected by atom probe tomography (APT). As already anticipated and in accordance with HR-TEM image in

Figure 2, APT shows that the fine-scale structure of bainitic ferrite is composed of carbon-depleted domains and carbon-enriched clusters, the latter with characteristic dimensions in the 5 nm range. Table 2 gathers, for different steels transforming to Super-Bainite at low temperature, the APT results regarding the amount of carbon in the matrix and the carbon content of the clusters. Here the ferrite matrix is considered as the low-carbon regions in the material where the solute atoms are randomly distributed (Rementeria, Poplawsky et al. 2017).

<Figure 3 near here>

Results in Table 2 show that in Super-Bainitic steels, ferrite matrix, measured away from carbon enriched features, is supersaturated with respect to the ferrite/austenite phase boundary under PE conditions (Caballero, Miller et al. 2010, Caballero, Miller et al. 2012). The same Table 2 indicates that, carbon saturation in ferrite tends to decrease as the transformation temperature is increased. On the other hand, and as expected, the average carbon composition in the as-quenched structure nearly matches the bulk composition of the alloy i.e., the structure is fully supersaturated. The disagreement between XRD and APT measurements in Table 2, is explained if we consider that XRD represents and average measurement of the low-carbon and high-carbon regions (i.e. clusters) in bainitic ferrite, while APT is a local measurement.

It has long been known that when displacive transformation of austenite takes place at temperatures below that ordered by Zener, the formed ferrite adopts a tetragonal crystalline structure (bct) centered on the body with carbon atoms located in one of the three subnets of interstices octahedral (Zener 1946). Carbon present in the parent phase is then trapped in the tetragonal lattice leading to a random distribution of carbon as in virgin martensite. However, at the temperatures where carbon mobility is higher, the aging of the structure is unavoidable and thermal activated reactions such as carbon segregation to lattice defects, carbon atom clustering and carbide precipitation soon take place (Lement, Averbach et al. 1954).

According to APT investigations (Rementeria, Capdevila et al. 2018), the composition of carbon clusters in super-bainitic structures is independent of the steel composition (see Table 2), and is close to the stoichiometric $Fe_{16}C_2$ compound (11.11 at.% C). It is remarkable that in naturally aged martensite, clusters have also a composition close to the stoichiometric $Fe_{16}C_2$ compound, although an ordered Fe_4C phase may be possible too (20 at.% C) (Taylor and Cohen 1992). The $Fe_{16}C_2$ compound can be described as being comprised of carbon situated in an ordered configuration on the octahedral sites of a tetragonally distorted bct-Fe lattice (Chang, Cerezo et al. 1984). Its origin seems to be associated with a redistribution of solute to lattice defects (Miller, Beaven et al. 1981).

In line with those results, and by means of positron lifetime spectroscopy, it has been possible to reveal the presence of a significant amount of mono-vacancies in Super-Bainite that could assist in retaining carbon in bainitic ferrite by the formation of C−vacancy complexes (Rementeria, Domínguez-Reyes et al. 2020). Due to the low mobility of these complexes in the ferrite, the complete partitioning of carbon towards the austenite/ferrite interface is hindered, and the phenomenon of carbon clustering in the ferritic phase formed at low temperature is promoted.

Clusters of this stoichiometry have been suggested to develop as pre-precipitates or embryos of carbides (Taylor, Chang et al. 1989). Originally, the absence of carbides particles inside the bainitic ferrite in TEM images of Super-Bainite as in Figure 1.b lead to the doubtful hypothesis that upper bainite was formed at these extremely low temperatures. However, the presence of intra-lath cementite was confirmed by APT in Super-Bainite (Caballero, Miller et al. 2014), and recently, it was established (Rementeria, Jimenez et al. 2017), by means of in-situ synchrotron high energy XRD, that both cementite and η−carbide do precipitate within bainite formed at low temperature. The η−carbide is a metastable product, unique of tempering reactions in carbon-supersaturated tetragonal matrices as those of martensite and bainitic ferrite.

Bhadeshia (Bhadeshia 1989) explained the detection of cementite instead of ε-carbide in lower bainite in terms of carbon trapping at dislocations following Kalish and Cohen (Kalish and Cohen 1970) tempering theory. Consistently, carbon trapped at dislocations was detected in Super-Bainite as carbon-enriched linear features by APT analysis, and examples of carbon atom maps showing carbon segregation to dislocations in bainitic ferrite are reported elsewhere (Caballero, Yen et al. 2011, Cornide, Miyamoto et al. 2011) (Taylor, Chang et al. 1989, Pereloma, Timokhina et al. 2006). The amount of carbon trapped at dislocations in Super-Bainite was measured by APT to vary from 6 to 14 at. % (Taylor, Chang et al. 1989) with no apparent correlation with the overall carbon content and the transformation temperature, but associated to its position relative to other defects (Pereloma, Timokhina et al. 2006, Cornide, Miyamoto et al. 2011). In any case, results suggest that the high dislocation density in Super-Bainite could have an effect on the free energy of carbon in the bainitic ferrite, suppressing ε-carbide formation during bainite reaction at low temperature.

<Table 3 near here>

Understanding the tensile properties of Super-Bainite

Exceptional hardness values (up to 700 HV), ultra-high strength values (up to 2 GPa) and, in some cases, exceptional total elongations of over 20% have been reported in Super-Bainite (Caballero and Bhadeshia 2004, Garcia-Mateo, Caballero et al. 2012, Sourmail, Caballero et al. 2013, Caballero, Garcia-Mateo et al. 2014). Table 3

summarizes some of these results for different alloys and heat treatments. The strength in these structures is conferred by a high fraction of nano-scale ferritic plates, the high density of defects, the intrinsic strength of the bct-Fe lattice and the complex carbon solute distribution observed by APT and partially illustrated in Figure 3. However, the deformation mechanisms operating in Super-Bainite, leading to an optimum combination of strength and ductility, are far from being understood.

<Figure 4 near here>

Similar to transformation induced plasticity (TRIP) assisted steels, in Super-Bainite the retained austenite can transform into martensite when subjected to mechanical stresses. The presence of plate martensite has been confirmed by TEM even at low deformation levels (Morales-Rivas, Yen et al. 2015). Figure 4 shows examples where the presence of twinned martensite formed during tensile test, has been identified at failure condition. In general, mechanically-induced martensitic transformation allows the necking instability to be delayed and thus, improves the elongation of the material. However, some retained austenite may remain untransformed even after failure of the specimens. The introduction of dislocations accumulating in the austenite can retard or even impede martensitic transformation by the phenomenon known as mechanical stabilization, in which such dislocations interferes with the movement of glissile martensite–austenite interfaces (Tsuzaki, Fukasaku et al. 1991, Chatterjee, Wang et al. 2006).

The complexity in explaining austenite stability arises from the fact that it depends on many interconnected factors, as its chemical composition, morphology and size. Generally speaking, low carbon content and a relatively large grain size of austenite might result in a low mechanical stability (Garcia-Mateo and Caballero 2005). Moreover, stability is also highly affected by the relative mechanical properties of the austenite and the surrounding phases, and the corresponding stress partitioning between them (Jacques, Furnémont et al. 2007).

Therefore, apart from the TRIP effect, the composite-type of strengthening plays a big role (Ryu, Kim et al. 2010). Under stress, in a composite microstructure, the plastic strain is initially focused in the more ductile soft phase, which then work-hardens; and eventually, the harder phase also deforms plastically. How can it be otherwise, the stress/strain partitioning depends on the individual mechanical properties of each phase i.e., bainitic ferrite and austenite, which in turn will be determined by the transformation temperature and time. In order to assess in which extend the phase transformation is the cause of the work-hardening mode, two super-bainitic structures transformed at two different temperatures (200 and 300 ºC), but containing the same percentage of austenite (35%) were investigated by in situ neutron diffraction during tensile testing at room temperature (Babu, Vogel et al. 2013).

In the microstructure obtained by transformation at 200 ºC, austenite mainly transformed at very early stage of deformation, 2%, and the sample broke at 3% deformation, being all the measured elongation uniform with no perceptible necking. By contrast, structure formed at 300ºC exhibited an uniform elongation of 10%, with no evidence of austenite to martensite transformation before necking. The analysis of each phase (amount and texture) as a function of the plastic strain revealed that, for the 200ºC microstructure, while bainitic ferrite hardly sustained any deformation, it was the austenite that assimilated most of the plastic deformation, which in turn lead to stress-assisted transformation to martensite. Such behavior has been recurrently detected for structures formed at 200 ºC and 220ºC (See Table 3) and being one of the main reasons for the low ductility of those microstructures. On the contrary, in samples heat treated at 300 ºC, both ferrite and austenite are capable of deforming by crystal rotation, allowing for a larger elongation. Hence, the strength mismatch between both phases seems to be an important issue to achieve large elongations.

Similarly, data in Table 3 clearly show that the increase of the transformation temperature results in enhancement of the total elongation. In other words, there seems to be beneficial to reduce the strength of the bainitic ferrite as the treatment temperature increases. Lan et al. (Lan, Liu et al. 2011) first showed that the nano-hardness of thin bainite platelets in Super-Bainite can exceed that of retained austenite as a result of the fine scale of the plates, and because of the excess carbon that they contain. Concurrently, nano-mechanical characterization of Super-Bainite using the combination of Atomic Force Microscopy (AFM) based techniques (Morales-Rivas, Gonzalez-Orive et al. 2015) revealed similar E values, close to 180 GPa, for both austenite and ferrite. Remarkably, these novel structures can be homogeneous in terms of Young's modulus despite its nanostructured nature. Under those circumstances, no mechanical partitioning between phases is expected within the elastic range of a tensile test. Instead, mechanical partitioning is likely to occur beyond the yield strength.

<Figure 5 near here>

On the other hand, the austenite twinning induced plasticity (TWIP) effect has been considered as a possible deformation mechanism. The formation of twins in austenite films has been identified as a strain hardening mechanism contributing to ductility in Super-Bainite (Morales-Rivas, Archie et al. 2018). Since the local carbon content in austenite has a direct influence on the stacking fault energy, TWIP is activated in these structures taking advantage of the heterogeneous carbon distribution in austenite with different morphologies and a wide range of austenitic grain sizes. TEM image in Figure 5.a reveals twins in a thin film of austenite in deformed samples after a high strain level. Some of these twins are considered to be accommodation twins, generated during bainite reaction in order to accommodate the shape change strain; but, also mechanical twins are observed with a second variant of twinning (inside circle). Electron

channeling contrast imaging (ECCI) revealed also at lower special resolution a higher presence of austenite twinning with the activation of a second twin system as the deformation takes place (see Figure 5.b). A Schmid factor analysis of the activated twin systems based on ECCI and electron backscatter diffraction (EBSD) (Morales-Rivas, Archie et al. 2018) results, allowed to conclude that new austenite mechanical twins are formed by the direct effect of the stress following the Schmid's law, whereas austenite accommodation twins have nucleated during displacive bainitic transformation and therefore would be closely related to the lattice invariant-strain and thus do not comply with the Schmid's law.

In-use properties and industrial application of Super-Bainite

Super-Bainite might offer an inexpensive solution for gears, windmill gearbox or even bearings for special applications (e.g. wind energy application) and mining parts based on their interesting combination of strength and toughness properties. Complex properties such as wear resistance and fatigue endurance have been assessed for the commercialization of super-bainitic steels (Sourmail, Caballero et al. 2013, Garcia-Mateo, Sourmail et al. 2014). In the context of rail applications, the rolling/sliding wear performance of several high silicon bainitic steels was investigated along with detailed microstructural characterization (Folgarait, Saccocco et al. 2004). Results revealed low wear rates of carbide-free bainitic steels and the beneficial effect that austenite embedded in the sub-micron ferritic structure has in controlling such property. In fact, Zhang et al. (Zhang, Zhang et al. 2011) found that super-bainitic steels show better wear resistance than much harder martensite. Likewise, Yang et al (Yang, Wang et al. 2012) observed an improvement in the material performance when the transformation temperature was such that the bainite was at the nano-scale.

These studies hint at considerable benefits of Super-Bainite against several wear and surface damage mechanisms. As anticipated, retained austenite is considered to be critical for improving wear resistance in these structures since this phase provides hardening by transformation into martensite (Leiro, Vuorinen et al. 2013, Das Bakshi, Leiro et al. 2014, Rementeria, García et al. 2015). It is well-known that hardness affects the stress needed to deform the material in the rolling/sliding contact, and it is a dominant factor in decreasing material loss. Wang et al. (Wang, Yang et al. 2008) found that the austenite in the vicinity of the sliding surface decomposes under the influence of high shear strains, into nano-grains of a ferritic phase of about 3 nm in size.

Regarding rotation-bending fatigue, Super-Bainite exhibits similar or lower fatigue strength compared to 100Cr6 in spite of somewhat lower UTS (Sourmail, Caballero et al. 2013). Microstructural examination by SEM and EBSD (Figure 6) below the fracture surface enabled the identification and nature of those boundaries deflecting the crack (Rementeria, Morales-Rivas et al. 2015). Results confirmed that the crack deflects at the interphase boundaries between blocks, packets and twins of the ferritic phase, but not to

a significant extent in the interphase boundaries within a single block. In addition, the block size was identified as the structure parameter controlling crack propagation. Unfortunately, the effect of austenite morphology and distribution on the fatigue strength of these structures is still uncertain due to the great difficulty in indexing by means of EBSD this phase when embedded in a nano-grained matrix (Rementeria, Morales-Rivas et al. 2015).

<Figure 6 near here>

In contrast, super-bainitic steels rolling contact fatigue (RCF) performance, of paramount importance in the context of bearings, has rarely been studied. Liu et al. (Liu, Sun et al. 2014) suggested that a microstructure composed of nanostructured bainite, martensite, and undissolved primary carbides with a hardness on par with commercial bearing steels (650-800 HV) can prolong up to 3.3 times the RCF life by effectively retarding crack initiation and propagation. However, the specific role of the different constituents was not addressed and the structures observed were not uniform. Later work by Solano-Alvarez et al. (Solano-Alvarez, Pickering et al. 2014) showed that the RCF damage in super-bainitic steels differs from that observed in conventional bearing steels. In particular, the formation of voids was prominent at interfaces between regions of bainitic ferrite and martensite, originated from the strain-induced transformation of the austenite blocks. Although void formation was identified as the key mechanism of damage evolution, cracks formed by the linking of voids generally exhibit considerable branching, delaying final fracture. Hence, different end-users have considered low temperature treatments such as austempering to develop bulk Super-Bainite in industrial parts required for rolling mill, crane and drill applications (Pujante, Casellas et al. 2019).

Similarly, bearing components have been manufactured with a specially designed steel grade that transforms to Super-Bainite, and have been tested under severe rolling conditions such as artificial pollution and compared to the 100Cr6 reference grade (Caballero, Pujante et al. 2019). Based on the results of the industrial trials, it was found that super-bainitic structures exhibits an optimum combination of contact fatigue and sliding wear performances. Such performance is explained by their ultra-fine grain size, ultra-high hardness, limited observed damage related to plasticity and the homogeneity of these structures. The designed steel showed competitive performance in terms of components lifetime on bearings industrial trials as well as a better endurance to artificial pollution test conditions.

On the other hand, surface modification on steels is well known to be beneficial for prolonging service life of components, and carburizing is one common process that can improve the surface hardness and wear resistance of steel by the diffusion of carbon atoms into the surface layers of the steel, such as on bearing and gear steels. Zhang et al.

(Zhang, Wang et al. 2008) firstly introduced Super-Bainite on the surface of carburizing 20CrMnMoNi steel by low-temperature austempering treatment, with a residual compressive stress of -196 MPa on the top surface of the carburized steel. Low-carbon martensite was obtained in the center. This microstructure combination exhibited a higher wear resistance and a higher fatigue life for rolling contact as compared with a martensitic reference steel (Zhang, Zhang et al. 2011, Zhang, Zhang et al. 2011, Zhang, Zhang et al. 2011).

More recently, Wang et al. (Wang, Yang et al. 2016) obtained a multiphase microstructure composed of Super-Bainite, martensite, undissolved spherical carbides and retained austenite on the top surface of carburizing 23Cr2Ni2Si1Mo steel after austempering at 200 °C, with a dual-phase microstructure of fine martensite lath and carbon-enriched retained austenite in the core. By austempering at such low temperatures, the core was subjected to a heat treatment process similar to the quenching and partitioning (Q&P) process, extensively investigated to improve the combination of high strength and adequate toughness of martensite steel. As compared with a conventional oil quenching and tempering structure, the low-temperature austempering specimens showed better stress conditions, higher wear resistance and higher interior toughness. Likewise, the RCF life of carburized steel was found to be superior to that of bulk high carbon nanostructured bainitic steel (Wang, Zhang et al. 2016), and it was attributed to different reasons: i) a finer carbide distribution observed in the top surface; ii) a deeper layer with higher residual compressive stress values in the carburizing samples; and iii) a higher work hardening ability detected by a larger amount of retained austenite transforming into martensite at the surface and a more stable untransformed retained austenite left in the top surface of the steel (Yang, Ji et al. 2018).

Two kinds of super-bainitic steels, G23Cr2Ni2Si1Mo and GCr15Si1Mo steels have recently been used to manufacture bearings, such as large bearings for high-powered and wind-driven generators and other heavy-duty equipment, as shown in Figure 7. These bearings manufactured by Luoyang LYC Bearing Co. in China exhibit excellent performance and have been accepted by the bearing industry. Such is the impact of the development, that these two new steels and the heat treatment process were included in the national standards of China (Ministry of Industry and Information Technology 2016, General Administration of Quality Supervision 2017, General Administration of Quality Supervision 2018).

<Figure 7 near here>

Nowadays, super-bainitic steels seem to be used in the manufacturing of bearings in China. The exploitation is considered to be an epoch-making technology, and this kind of bearing has been termed ‘‘the second generation of bainitic bearing” by the Chinese

bearing industry. This achievement has been defined as ‘the progress of China’s bearing manufacturing industry, as China leads the world in the development of nanostructured bainitic bearing steels’ (Zhang and Yang 2019).

Future Challenges

Despite all the developments and efforts place into accelerating the bainitic transformation in Super-Bainitic steels, the required long treatments, and its associated costs, remains as a drawback for its implementation in a wider range of markets. In this sense, new approaches are here proposed for the alloy design of the base material to ensure the scientific and technical feasibility of the proposed work.

Although some of the revised approaches in this work, have proven to shorten the transformation time of Super-Bainite below 10 hours, the applicability of these processes still needs to be verified, since there is no unified and objective criterion that allows to determine the end of the bainitic transformation, and therefore a meaningful comparison of results is difficult (Santajuana, Eres-Castellanos et al. 2019). Likewise, 10 h is still longer than the time needed for manufacturing more of the industrial components, which is around 4-6 hours, and developing shorter heat treatment process for super-bainitic parts remains as an important task. In addition, the kinetics reaction considering incubation and transformation stages should be quantitative assessed in order to realize a shortened transformation time.

Adjusting the chemical composition with microalloying additions and the introduction of particles is expected to accelerate bainite reaction at low temperatures. Microalloying treatment and/or the introduction of particles with an extremely low mismatch with ferrite, such as a rare kind of nitride—vanadium nitride (VN), is another potential method to deal with this disadvantage. Thus, (Garcia-Mateo, Cornide et al. 2008) found that the precipitation of V(C,N) effectively enhanced acicular ferrite formation by strongly increasing the ratio between intragranular and grain boundary nucleation sites in a low-carbon steel. Recently, He et al. (He, Xu et al. 2017) showed that the bainitic transformation kinetics were accelerated in a low-carbon steel with the addition of B after ausforming, although there is the wide spread belief that B retards the bainitic transformation kinetics. Choosing and controlling microalloying additions and/or the introduction of particles as well as via an optimal process should be further studied in detail.

Other physical metallurgy issues, limiting Super-Bainite commercialization, that require further consideration and study of certain scientific fundaments are, the stability of retained austenite and its actual effect on the dimensional stability of components; the role of residual cementite on in-use properties; the fatigue mechanism under conditions of high rotation speed and/or heavy load; and the microstructural evolution during the fatigue process (Zhang and Yang 2019).

References

Babu, S. S., S. Vogel, C. Garcia-Mateo, B. Clausen, L. Morales-Rivas and F. G. Caballero (2013). "Microstructure evolution during tensile deformation of a nanostructured bainitic steel." Scripta Materialia **69**(11-12): 777-780.

Bhadeshia, H. K. D. H. (1989). "Theoretical-Analysis of Changes in Cementite Composition During Tempering of Bainite." Materials Science and Technology **5**(2): 131-137.

Bhadeshia, H. K. D. H. (2015). Bainite in Steels. Transformations, Microstructure and Properties. London, Institute of Materials, Minerals and Mining.

Bhadeshia, H. K. D. H. and D. V. Edmonds (1979). "The bainite transformation in a silicon steel." Metallurgical Transactions A **10**(7): 895-907.

Bhadeshia, H. K. D. H. and R. W. K. Honeycombe (2006). Steels: Microstructure And Properties, Butterworths-Heinemann (Elsevier).

Caballero, F. G. and H. K. D. H. Bhadeshia (2004). "Very strong bainite." Current Opinion in Solid State and Materials Science **8**(3-4): 251-257.

Caballero, F. G., C. Garcia-Mateo and M. K. Miller (2014). "Design of Novel Bainitic Steels: Moving from UltraFine to Nanoscale Structures." JOM **66**(5): 747-755.

Caballero, F. G., C. Garcia-Mateo, M. J. Santofimia, M. K. Miller and C. Garcia de Andres (2009). "New experimental evidence on the incomplete transformation phenomenon in steel." Acta Materialia **57**(1): 8-17.

Caballero, F. G., M. K. Miller and C. Garcia-Mateo (2010). "Carbon supersaturation of ferrite in a nanocrystalline bainitic steel." Acta Materialia **58**(7): 2338-2343.

Caballero, F. G., M. K. Miller and C. Garcia-Mateo (2014). "Influence of transformation temperature on carbide precipitation sequence during lower bainite formation." Materials Chemistry and Physics **146**(1-2): 50-57.

Caballero, F. G., M. K. Miller, C. Garcia-Mateo, J. Cornide and M. J. Santofimia (2012). "Temperature dependence of carbon supersaturation of ferrite in bainitic steels." Scripta Materialia **67**(10): 846-849.

Caballero, F. G., J. Pujante, T. Sourmail, R. Rementeria, D. De-castro, P. Dierickx, G. Ramírez, C. Sidoroff-coicaud, P. V. Moghaddam and E. Vuorinen (2019). "Advanced heat treatments and complex ferritic structures for bearing steels." Metals **9**(11).

Caballero, F. G., H.-W. Yen, M. K. Miller, J.-R. Yang, J. Cornide and C. Garcia-Mateo (2011). "Complementary use of transmission electron microscopy and atom probe tomography for the examination of plastic accommodation in nanocrystalline bainitic steels." Acta Materialia **59**(15): 6117-6123.

Chang, L., A. Cerezo, G. Smith, D.W., M. Miller, K., M. Burke, G., S. Brenner, S., K. Taylor, A., T. Abe and G. Olson, B. (1984). "AGEING OF Fe-Ni-C MARTENSITE." J. Phys. Colloques **45**(C9): C9-409-C409-416.

Chang, L. C. and H. K. D. H. Bhadeshia (1995). "Metallographic Observations Of Bainite Transformation Mechanism." Materials Science and Technology **11**(2): 105-108.

Chatterjee, S., H. S. Wang, J. R. Yang and H. K. D. H. Bhadeshia (2006). "Mechanical stabilisation of austenite." Materials Science and Technology **22**(6): 641-644.

Christian, J., W., G. Olson, B. and M. Cohen (1995). "Classification of Displacive Transformations : What is a Martensitic Transformation ?" J. Phys. IV Colloque **05**(C8): C8-3-C8-10.

Christian, J. W. (1958). "Accommodation Strains in Martensite Formation, and the Use of a Dilatation Parameter." Acta Metallurgica **6**(5): 377-379.

Cornide, J., C. Garcia-Mateo, C. Capdevila and F. G. Caballero (2013). "An assessment of the contributing factors to the nanoscale structural refinement of advanced bainitic steels." Journal of Alloys and Compounds **577**: S43-S47.

Cornide, J., G. Miyamoto, F. G. Caballero, T. Furuhara, M. K. Miller and C. Garcia-Mateo (2011). "Distribution of dislocations in nanostructured bainite." Solid State Phenomena **172-174**: 117-122.

Das Bakshi, S., A. Leiro, B. Prakash and H. K. D. H. Bhadeshia (2014). "Dry rolling/sliding wear of nanostructured bainite." Wear **316**(1-2): 70-78.

De-Castro, D., R. Rementeria, J. Vivas, T. Sourmail, J. D. Poplawsky, E. Urones-Garrote, J. A. Jimenez, C. Capdevila and F. G. Caballero (2020). "Examining the multi-scale complexity and the crystallographic hierarchy of isothermally treated bainitic and martensitic structures." Materials Characterization **160**.

Erb, U., G. Palumbo and J. L. McCrea (2011). 5 - The processing of bulk nanocrystalline metals and alloys by electrodeposition. Nanostructured Metals and Alloys. S. H. Whang, Woodhead Publishing**:** 118-151.

Eres-Castellanos, A., L. Morales-Rivas, A. Latz, F. G. Caballero and C. Garcia-Mateo (2018). "Effect of ausforming on the anisotropy of low temperature bainitic transformation." Materials Characterization **145**: 371-380.

Fang, K., J. Yang, D. Zhao, K. Song, Z. Yan and H. Fang (2012). Review of nanobainite steel welding. Advanced Materials Research. **482-484:** 2405-2408.

Folgarait, P., A. Saccocco, A. De Ro and B. Eisenkolb (2004). Bainitic steels for new rail materials. Ref 7210-PR/290, European Commission, Luxembourg, Int. (Revue).

Garcia-Mateo, C. and F. G. Caballero (2005). "The role of retained austenite on tensile properties of steels with bainitic microstructures." Materials Transactions **46**(8): 1839-1846.

Garcia-Mateo, C., F. G. Caballero and H. K. D. H. Bhadeshia (2003). "Acceleration of Low-temperature Bainite." ISIJ International **43**(11): 1821-1825.

Garcia-Mateo, C., F. G. Caballero, T. Sourmail, M. Kuntz, J. Cornide, V. Smanio and R. Elvira (2012). "Tensile behaviour of a nanocrystalline bainitic steel containing 3 wt% silicon." Materials Science and Engineering a-Structural Materials Properties Microstructure and Processing **549**: 185-192.

Garcia-Mateo, C., J. Cornide, C. Capidevila, F. G. Caballero and C. Garcia de Andres (2008). "Influence of V precipitates on acicular ferrite transformation Part 2: Transformation kinetics." Isij International **48**(9): 1276-1279.

Garcia-Mateo, C., J. A. Jimenez, H. W. Yen, M. K. Miller, L. Morales-Rivas, M. Kuntz, S. P. Ringer, J. R. Yang and F. G. Caballero (2015). "Low temperature bainitic ferrite: Evidence of carbon super-saturation and tetragonality." Acta Materialia **91**: 162-173.

Garcia-Mateo, C., G. Paul, M. Somani, D. Porter, L. Bracke, A. Latz, C. Garcia De Andres and F. Caballero (2017). "Transferring Nanoscale Bainite Concept to Lower C Contents: A Perspective." Metals **7**(5): 159.

Garcia-Mateo, C., G. Paul, M. C. Somani, D. A. Porter, L. Bracke, A. Latz, C. Garcia De Andres and F. G. Caballero (2017). "Transferring Nanoscale Bainite Concept to Lower C Contents: A Perspective." Metals **7**(5).

Garcia-Mateo, C., T. Sourmail, F. G. Caballero, V. Smanio, M. Kuntz, C. Ziegler, A. Leiro, E. Vuorinen, R. Elvira and T. Teeri (2014). "Nanostructured steel industrialisation: plausible reality." Materials Science and Technology **30**(9): 1071-1078.

General Administration of Quality Supervision, I. a. Q. o. t. P. s. R. o. C. (2018). Rolling bearings-Parts made from high-carbon chromium bearing steels-Specifications for heat treatment (GB/T 34891). People's Republic of China.

General Administration of Quality Supervision, I. a. Q. o. t. P. s. R. o. C., Standardization Administration of the People's Republic of China (2017). Carburizing steels for bearing (GB/T 3203-2016). People's Republic of China.

Gong, W., Y. Tomota, Y. Adachi, A. M. Paradowska, J. F. Kelleher and S. Y. Zhang (2013). "Effects of ausforming temperature on bainite transformation, microstructure and variant selection in nanobainite steel." Acta Materialia **61**(11): 4142-4154.

Gong, W., Y. Tomota, M. S. Koo and Y. Adachi (2010). "Effect of ausforming on nanobainite steel." Scripta Materialia **63**(8): 819-822.

Han, K., M. J. van Genderen, A. Böttger, H. W. Zandbergen and E. J. Mittemeijer (2001). "Initial stages of Fe-C martensite decomposition." Philosophical Magazine A **81**(3): 741-757.

He, B., W. Xu and M. Huang (2017). "Effect of boron on bainitic transformation kinetics after ausforming in low carbon steels." Journal of Materials Science & Technology **33**(12): 1494-1503.

He, J., A. Zhao, Y. Huang, C. Zhi and F. Zhao (2015). Acceleration of Bainite Transformation at Low Temperature by Warm Rolling Process. Materials Today: Proceedings, Elsevier Ltd.

He, J., A. Zhao, C. Zhi and H. Fan (2015). "Acceleration of nanobainite transformation by multi-step ausforming process." Scripta Materialia **107**(0): 71-74.

Hulme-Smith, C. N., I. Lonardelli, A. C. Dippel and H. K. D. H. Bhadeshia (2013). "Experimental evidence for non-cubic bainitic ferrite." Scripta Materialia **69**(5): 409-412.

Humphreys, F. J., P. B. Prangnell and R. Priestner (2001). "Fine-grained alloys by thermomechanical processing." Current Opinion in Solid State and Materials Science **5**(1): 15-21.

Jacques, P. J., Q. Furnémont, F. Lani, T. Pardoen and F. Delannay (2007). "Multiscale mechanics of TRIP-assisted multiphase steels: I. Characterization and mechanical testing." Acta Materialia **55**(11): 3681-3693.

Kalish, D. and M. Cohen (1970). "Structural changes and strengthening in the strain tempering of Martensite." Materials Science and Engineering **6**: 156-166.

Krauss, G. (2005). Steels: Processing, structure, and performance (Second Edition). Materials Park, USA, ASM International.

Kusunoki, M. and S. Nagakura (1981). "Modulated structure of iron-carbon martensite studied by electron microscopy and diffraction." Journal of Applied Crystallography **14**(5): 329-336.

Lan, H. F., X. H. Liu and L. X. Du (2011). "Ultra-hard bainitic steels processed through low temperature heat treatment." Advanced Materials Research **156-157**: 1708-1712.

Leiro, A., E. Vuorinen, K. G. Sundin, B. Prakash, T. Sourmail, V. Smanio, F. G. Caballero, C. Garcia-Mateo and R. Elvira (2013). "Wear of nano-structured carbide-free bainitic steels under dry rolling-sliding conditions." Wear **298**: 42-47.

Lement, B. S., B. L. Averbach and M. Cohen (1954). "Microstructural Changes On Tempering Iron Carbon Alloys." Transactions of the American Society for Metals **46**: 851-881.

Li, Q., X. Huang and W. Huang (2016). "Microstructure and mechanical properties of a medium-carbon bainitic steel by a novel quenching and dynamic partitioning (Q-DP) process." Materials Science and Engineering A **662**: 129-135.

Liu, H., J. Sun, T. Jiang, S. Guo and Y. Liu (2014). "Improved rolling contact fatigue life for an ultrahigh-carbon steel with nanobainitic microstructure." Scripta Materialia **90**(1): 17-20.

Miller, M. K., P. A. Beaven and G. D. W. Smith (1981). "STUDY OF THE EARLY STAGES OF TEMPERING OF IRON-CARBON MARTENSITES BY ATOM PROBE FIELD ION MICROSCOPY." Metallurgical transactions. A, Physical metallurgy and materials science **12 A**(7): 1197-1204.

Ministry of Industry and Information Technology, P. s. R. o. C. (2016). Bearing steel rolling ring and blank (YB/T 4572). People's Republic of China.

Morales-Rivas, L., F. Archie, S. Zaefferer, M. Benito-Alfonso, S.-P. Tsai, J.-R. Yang, D. Raabe, C. Garcia-Mateo and F. G. Caballero (2018). "Crystallographic examination of the interaction between texture evolution, mechanically induced martensitic transformation and twinning in nanostructured bainite." Journal of Alloys and Compounds **752**: 505-519.

Morales-Rivas, L., A. Gonzalez-Orive, C. Garcia-Mateo, A. Hernandez-Creus, F. G. Caballero and L. Vazquez (2015). "Nanomechanical characterization of nanostructured bainitic steel: Peak Force Microscopy and Nanoindentation with AFM." Scientific Reports **5**.

Morales-Rivas, L., H.-W. Yen, B.-M. Huang, M. Kuntz, F. G. Caballero, J.-R. Yang and C. Garcia-Mateo (2015). "Tensile Response of Two Nanoscale Bainite Composite-Like Structures." JOM Journal of the Minerals Metals and Materials Society **67**(10): 2223-2235.

Morito, S., X. Huang, T. Furuhara, T. Maki and N. Hansen (2006). "The morphology and crystallography of lath martensite in alloy steels." ACTA MATERIALIA **54**(19): 5323-5331.

Ohmori, Y., H. Ohtsubo, Y. C. Jung, S. Okaguchi and H. Ohtani (1994). "Morphology of bainite and widmanstätten ferrite." Metallurgical and Materials Transactions A **25**(9): 1981-1989.

Pereloma, E. V. (2016). "Critical assessment 20: on carbon excess in bainitic ferrite." Materials Science and Technology **32**(2): 99-103.

Pereloma, E. V., I. B. Timokhina, J. J. Jonas and M. K. Miller (2006). "Fine-scale microstructural investigations of warm rolled low-carbon steels with and without Cr, P, and B additions." Acta Materialia **54**(17): 4539-4551.

Pujante, J., D. Casellas, T. Sourmail, F. G. Caballero, R. Rementeria, A. Soto, J. M. Llanos, E. Vuorinen, B. Prakash, J. Hardell, P. Valizadeh Moghaddam, D. Dietrich and P. Ferrer (2019). Novel Nano-Structured Bainitic Steels for Enhanced Durability of Wear Resistant Components: Microstructural Optimisation through Simulative Wear and Field Tests (BAINWEAR). RFSR-CT-2014-00016. Luxembourg, European Commission.

Rementeria, R., C. Capdevila, R. Dominguez-Reyes, J. D. Poplawsky, W. Guo, E. Urones-Garrote, C. Garcia-Mateo and F. G. Caballero (2018). "Carbon Clustering in Low-Temperature Bainite." Metallurgical and Materials Transactions a-Physical Metallurgy and Materials Science **49A**(11): 5277-5287.

Rementeria, R., R. Domínguez-Reyes, C. Capdevila, C. Garcia-Mateo and F. G. Caballero (2020). "Positron Annihilation Spectroscopy Study of Carbon-Vacancy Interaction in Low-Temperature Bainite." Scientific Reports **10**(1).

Rementeria, R., I. García, M. M. Aranda and F. G. Caballero (2015). "Reciprocating-sliding wear behavior of nanostructured and ultra-fine high-silicon bainitic steels." Wear **338-339**: 202-209.

Rementeria, R., J. A. Jimenez, S. Y. P. Allain, G. Geandier, J. D. Poplawsky, W. Guo, E. Urones-Garrote, C. Garcia-Mateo and F. G. Caballero (2017). "Quantitative assessment of carbon allocation anomalies in low temperature bainite." Acta Materialia **133**: 333-345.

Rementeria, R., L. Morales-Rivas, M. Kuntz, C. Garcia-Mateo, E. Kerscher, T. Sourmail and F. G. Caballero (2015). "On the role of microstructure in governing the fatigue behaviour of nanostructured bainitic steels." Materials Science and Engineering a-Structural Materials Properties Microstructure and Processing **630**: 71-77.

Rementeria, R., J. D. Poplawsky, M. M. Aranda, W. Guo, J. A. Jimenez, C. Garcia-Mateo and F. G. Caballero (2017). "Carbon concentration measurements by atom probe tomography in the ferritic phase of high-silicon steels." Acta Materialia **125**: 359-368.

Ryu, J. H., D.-I. Kim, H. S. Kim, H. K. D. H. Bhadeshia and D.-W. Suh (2010). "Strain partitioning and mechanical stability of retained austenite." Scripta Materialia **63**(3): 297-299.

Santajuana, M. A., A. Eres-Castellanos, V. Ruiz-Jimenez, S. Allain, G. Geandier, F. G. Caballero and C. Garcia-Mateo (2019). "Quantitative assessment of the time to end bainitic transformation." Metals **9**(9).

Singh, S. B. and H. K. D. H. Bhadeshia (1998). "Estimation of bainite plate-thickness in low-alloy steels." Materials Science and Engineering A **245**(1): 72-79.

Solano-Alvarez, W., E. J. Pickering and H. K. D. H. Bhadeshia (2014). "Degradation of nanostructured bainitic steel under rolling contact fatigue." Materials Science and Engineering: A **617**(0): 156-164.

Sourmail, T., F. G. Caballero, C. Garcia-Mateo, V. Smanio, C. Ziegler, M. Kuntz, R. Elvira, A. Leiro, E. Vuorinen and T. Teeri (2013). "Evaluation of potential of high Si high C steel nanostructured bainite for wear and fatigue applications." Materials Science and Technology **29**(10): 1166-1173.

Swallow, E. and H. K. D. H. Bhadeshia (1996). "High resolution observations of displacements caused by bainitic transformation." Materials Science and Technology **12**(2): 121-125.

Takayama, N., G. Miyamoto and T. Furuhara (2012). "Effects of transformation temperature on variant pairing of bainitic ferrite in low carbon steel." ACTA MATERIALIA **60**(5): 2387-2396.

Taylor, K. A., L. Chang, G. B. Olson, G. D. W. Smith, M. Cohen and J. B. Vandersande (1989). "Spinodal Decomposition During Aging Of Fe-Ni-C Martensites." METALLURGICAL TRANSACTIONS A-PHYSICAL METALLURGY AND MATERIALS SCIENCE **20**(12): 2717-2737.

Taylor, K. A. and M. Cohen (1992). "Aging of ferrous martensites." Progress in Materials Science **36**: 151-272.

Timokhina, I., H. Beladi, X. Xiong and P. Hodgson (2011). "Effect of Composition and Processing Parameters on the Formation of Nano-Bainite in Advanced High Strength Steels." Journal of Iron and Steel Research International **18**: 238-241.

Tsuzaki, K., S.-i. Fukasaku, Y. Tomota and T. Maki (1991). "Effect of prior deformation of austenite on the $\gamma \rightarrow \varepsilon$ martensitic transformation in Fe-Mn alloys." Materials Transactions, JIM **32**(3): 222-228.

Valiev, R. Z. (2011). Producing bulk nanostructured metals and alloys by severe plastic deformation (SPD). Nanostructured Metals and Alloys. S. H. Whang, Woodhead Publishing**:** 3-39.

Wang, T. S., J. Yang, C. J. Shang, X. Y. Li, B. Lv, M. Zhang and F. C. Zhang (2008). "Sliding friction surface microstructure and wear resistance of 9SiCr steel with low-temperature austempering treatment." Surface and Coatings Technology **202**(16): 4036-4040.

Wang, X. L., K. M. Wu, F. Hu, L. Yu and X. L. Wan (2014). "Multi-step isothermal bainitic transformation in medium-carbon steel." Scripta Materialia **74**: 56-59.

Wang, Y., Z. Yang, F. Zhang and D. Wu (2016). "Microstructures and mechanical properties of surface and center of carburizing 23Cr2Ni2Si1Mo steel subjected to low-temperature austempering." Materials Science and Engineering: A **670**: 166-177.

Wang, Y., F. Zhang, Z. Yang, B. Lv and C. Zheng (2016). "Rolling Contact Fatigue Performances of Carburized and High-C Nanostructured Bainitic Steels." Materials **9**(12): 960.

Whang, S. H. (2011). Nanostructured metals and alloys: Processing, microstructure, mechanical properties and applications Introduction. Cambridge, Woodhead Publ Ltd.

Yang, H. S. and H. K. D. H. Bhadeshia (2008). "Designing low carbon, low temperature bainite." Materials Science and Technology **24**(3): 335-342.

Yang, J., T. S. Wang, B. Zhang and F. C. Zhang (2012). "Sliding wear resistance and worn surface microstructure of nanostructured bainitic steel." Wear **282-283**: 81-84.

Yang, Z. N., Y. L. Ji, F. C. Zhang, M. Zhang, B. Nawaz and C. L. Zheng (2018). "Microstructural evolution and performance change of a carburized nanostructured bainitic bearing steel during rolling contact fatigue process." Materials Science and Engineering: A **725**: 98-107.

Zener, C. (1946). "Kinetics of The Decomposition Of Austenite." Transactions of the American Institute of Mining and Metallurgical Engineers **167**: 550-595.

Zhang, F. and Z. Yang (2019). "Development of and Perspective on High-Performance Nanostructured Bainitic Bearing Steel." Engineering **5**(2): 319-328.

Zhang, F. C., T. S. Wang, P. Zhang, C. L. Zheng, B. Lv, M. Zhang and Y. Z. Zheng (2008). "A novel method for the development of a low-temperature bainitic microstructure in the surface layer of low-carbon steel." Scripta Materialia **59**(3): 294-296.

Zhang, M., T. S. Wang, Y. H. Wang, J. Yang and F. C. Zhang (2013). "Preparation of nanostructured bainite in medium-carbon alloysteel." Materials Science and Engineering: A **568**: 123-126.

Zhang, M., Y. H. Wang, C. L. Zheng, F. C. Zhang and T. S. Wang (2014). "Austenite deformation behavior and the effect of ausforming process on martensite starting temperature and ausformed martensite microstructure in medium-carbon Si-Al-rich alloy steel." Materials Science and Engineering A **596**: 9-14.

Zhang, M., Y. H. Wang, C. L. Zheng, F. C. Zhang and T. S. Wang (2014). "Effects of ausforming on isothermal bainite transformation behaviour and microstructural refinement in medium-carbon Si-Al-rich alloy steel." Materials and Design **62**: 168-174.

Zhang, P., F. C. Zhang and T. S. Wang (2011). "Preparation and microstructure characteristics of low-temperature bainite in surface layer of low carbon gear steel." Applied Surface Science **257**(17): 7609-7614.

Zhang, P., F. C. Zhang, Z. G. Yan, T. S. Wang and L. H. Qian (2011). "Rolling contact fatigue property of low-temperature bainite in surface layer of a low carbon steel." Materials science Forums **675-677**: 585-588.

Zhang, P., F. C. Zhang, Z. G. Yan, T. S. Wang and L. H. Qian (2011). "Wear property of low-temperature bainite in the surface layer of a carburized low carbon steel." Wear **271**(5): 697-704.

Zhao, L., L. Qian, J. Meng, Q. Zhou and F. Zhang (2016). "Below-Ms austempering to obtain refined bainitic structure and enhanced mechanical properties in low-C high-Si/Al steels." Scripta Materialia **112**: 96-100.

Table Captions

Table 1 Chemical composition of super-bainitic steels, wt.%. (Caballero and Bhadeshia 2004, Caballero, Garcia-Mateo et al. 2014).

Table 2 Tetragonality values and carbon content in ferrite determined by X-ray diffraction (XRD) analysis of Super-Bainite formed at different temperatures and times in comparison with martensite (as-quench sample) and tempered martensite (Quenched and tempered, Q&T, sample); and corresponding atom probe tomography (APT) data measured randomly distributed and as carbon clusters in bainitic ferrite.

Table 3. Hardness values and tensile properties of Super-Bainite (Caballero and Bhadeshia 2004, Garcia-Mateo, Caballero et al. 2012, Sourmail, Caballero et al. 2013, Caballero, Garcia-Mateo et al. 2014).

Figure Captions

Figure 1: (a) SEM and (b, c) TEM images of Super-Bainite formed at 220 °C; α is bainitic ferrite, and γ is retained austenite.

Figure 2: (a) HR-TEM image and (b) corresponding FFT taken in ferrite of Super-Bainite formed at 250ºC.

Figure 3: Clusters noticeable by carbon iso-concentration surfaces at 4 at.% C superimposed with the carbon atom map in bainitic ferrite formed at 230 °C in Fe-4.3C-5.4Si-0.8Mn-0.4Cr at.% steel (Fe-1.0C-2.9Si-0.8Mn-0.4Cr wt.%).

Figure 4: Bright field (BF) TEM images of twinned martensite within an austenite block in Super-Bainite at failure condition.

Figure 5: (a) Bright field micrograph of mechanical twins in austenite in Super-Bainite at 220 °C and deformed up to 6% strain; (b) ECCI micrograph of austenite block showing twinning after deformation at 3% strain.

Figure 6: Ferrite Inverse Pole Figure (IPF) map showing crystallographic boundaries of microstructure of Super-Bainite treated at 270 °C below the fracture surface of a fatigue sample.

Figure 7: (a) The main shaft bearing and (b) the pitch bearing for a high-power wind turbine, made by Luoyang LYC Bearing Co., Ltd. The outer diameter and inner diameters of the main shaft bearing are 3200 mm and 2620 mm, respectively, and those of the yaw bearing are 5107 mm and 4420 mm, respectively (Zhang and Yang 2019).

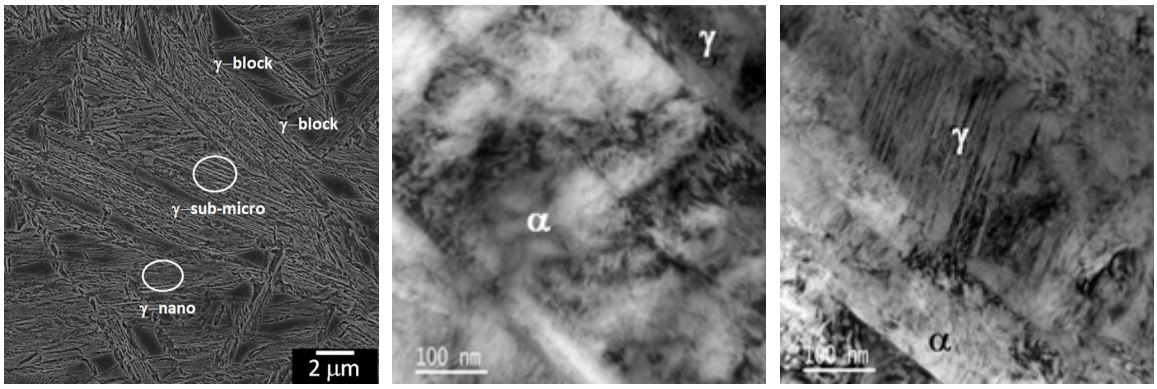

(a) (b) (c)

Figure 1: (a) SEM and (b, c) TEM images of Super-Bainite formed at 220 °C; α is bainitic ferrite, and γ is retained austenite.

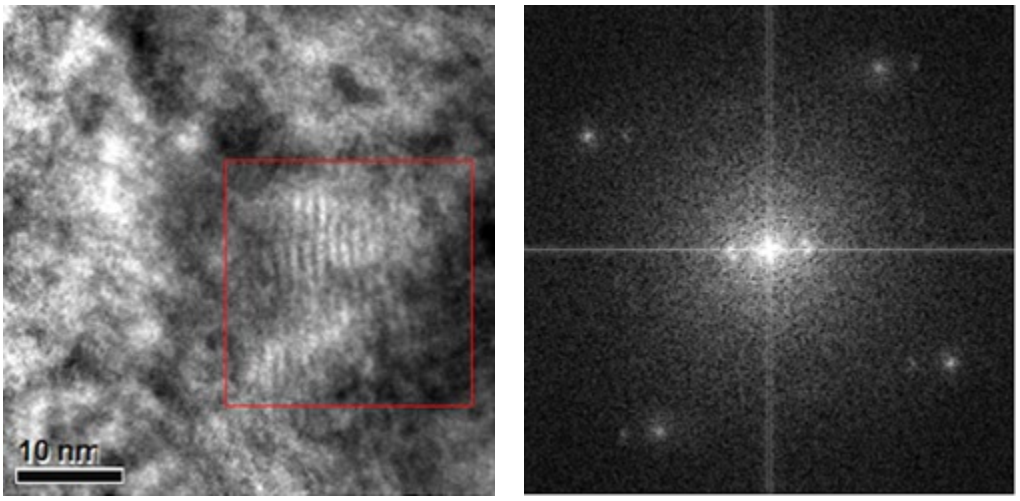

(a) (b)

Figure 2: (a) HR-TEM image and (b) corresponding FFT taken in ferrite of Super-Bainite formed at 250ºC.

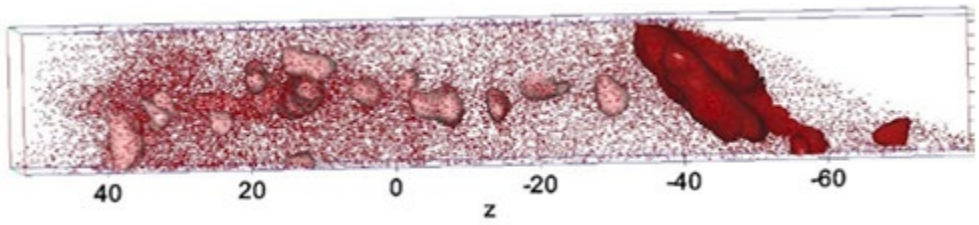

Figure 3: Clusters noticeable by carbon iso-concentration surfaces at 4 at.% C superimposed with the carbon atom map in bainitic ferrite formed at 230 °C in Fe-4.3C-5.4Si-0.8Mn-0.4Cr at.% steel (Fe-1.0C-2.9Si-0.8Mn-0.4Cr wt.%).

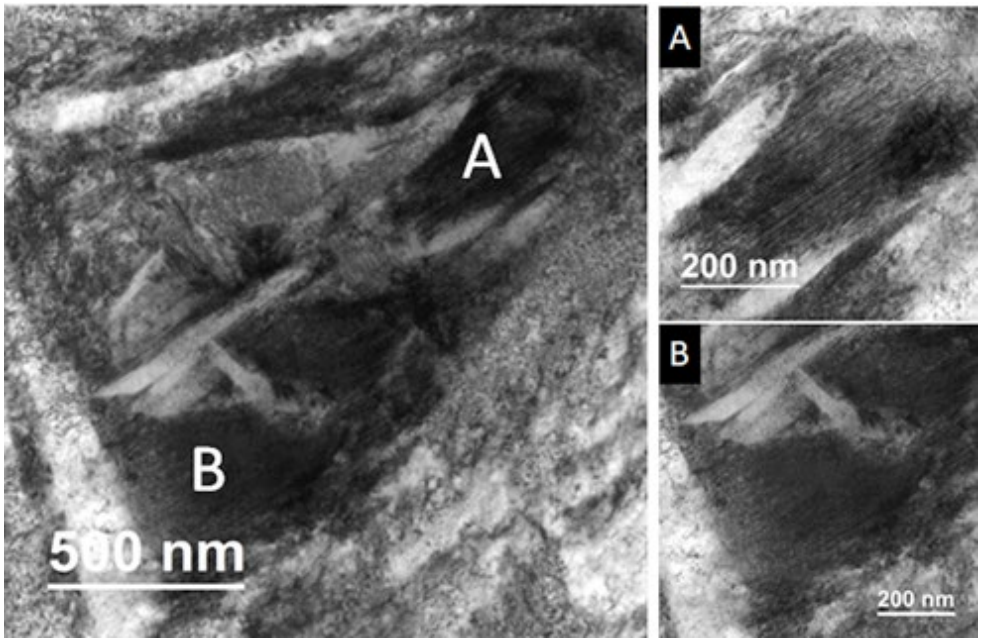

Figure 4: Bright field (BF) TEM images of twinned martensite within an austenite block in Super-Bainite at failure condition.

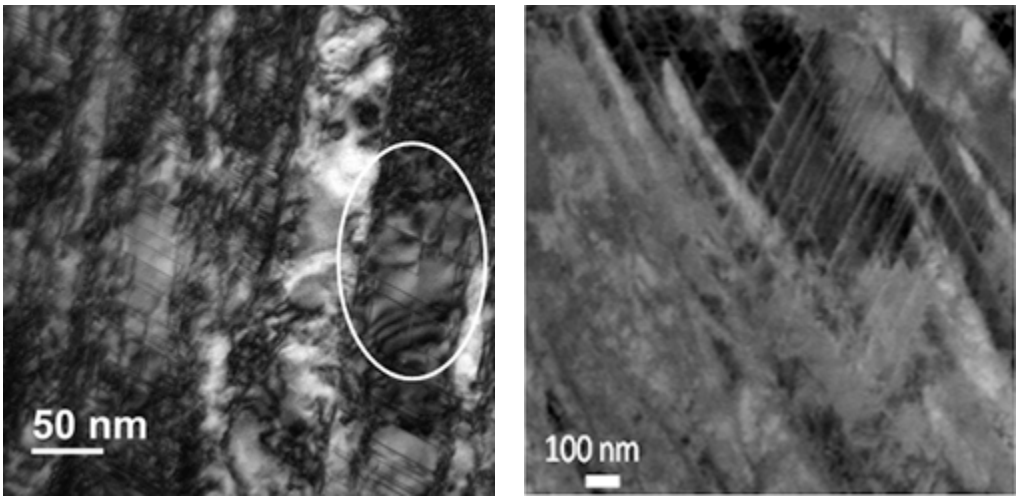

(a) (b)

Figure 5: (a) Bright field micrograph of mechanical twins in austenite in Super-Bainite at 220 °C and deformed up to 6% strain; (b) ECCI micrograph of austenite block showing twinning after deformation at 3% strain.

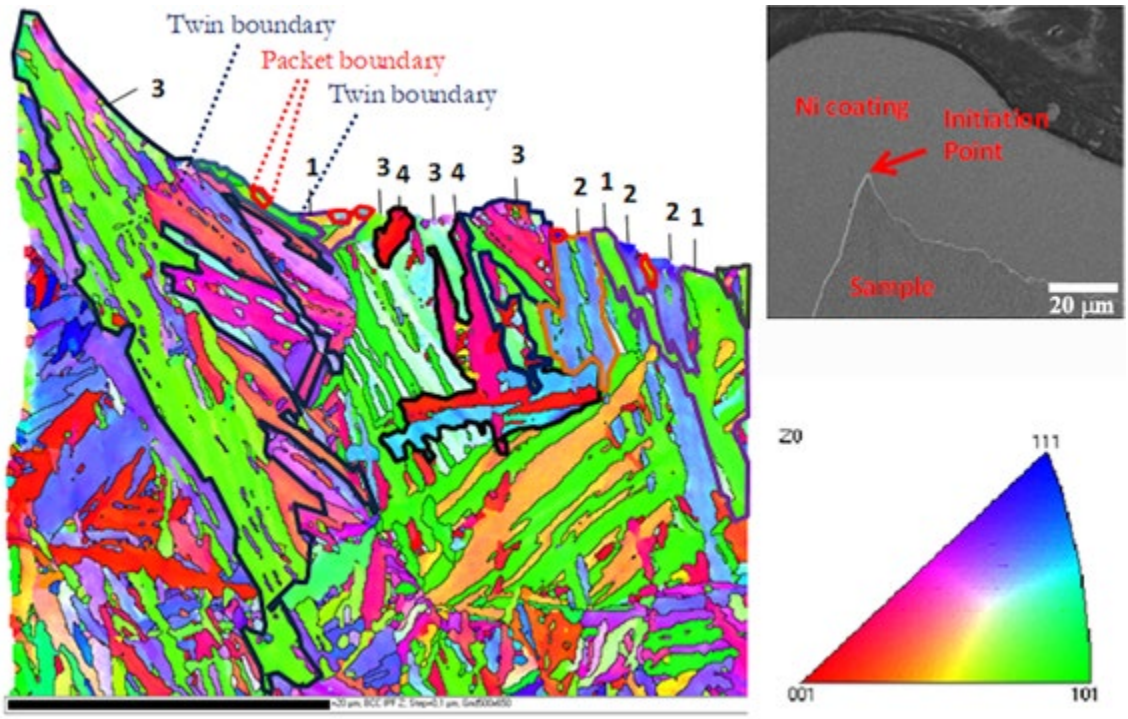

Figure 6: Ferrite Inverse Pole Figure (IPF) map showing crystallographic boundaries of microstructure of Super-Bainite treated at 270 °C below the fracture surface of a fatigue sample.

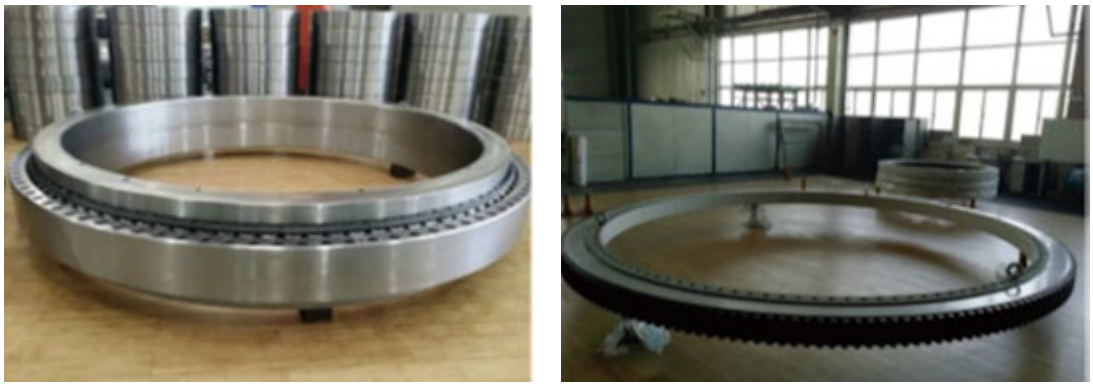

(a) (b)

Figure 7: (a) The main shaft bearing and (b) the pitch bearing for a high-power wind turbine, made by Luoyang LYC Bearing Co., Ltd. The outer diameter and inner diameters of the main shaft bearing are 3200 mm and 2620 mm, respectively, and those of the yaw bearing are 5107 mm and 4420 mm, respectively (Zhang and Yang 2019).

Table 1 Chemical composition of super-bainitic steels, wt.%. (Caballero and Bhadeshia 2004, Caballero, Garcia-Mateo et al. 2014).

Steel	C	Si	Mn	Cr	Mo	V	Nb	Co	Al
First Generation:									
Super-Bainite 0	0.79	1.59	1.94	1.33	0.30	0.11	-	-	-
Super-Bainite 1	0.98	1.46	1.89	1.26	0.29	0.09			
Super-Bainite 2	0.83	1.57	1.98	1.02	0.24	-	-	1.54	-
Super-Bainite 3	0.78	1.49	1.95	0.97	0.24	-	-	1.60	0.99
Second Generation:									
Super-Bainite 4	0.99	1.58	0.76	0.45	-	-	-	-	-
Super-Bainite 5	1.00	1.53	0.75	0.51	-	-	0.02	-	-
Super-Bainite 6	1.01	1.51	0.82	0.46	0.10	-	-	-	-
Super-Bainite 7	0.98	2.90	0.77	0.45	-	-	-	-	-
Super-Bainite 8	0.88	1.54	0.69	0.50	-	-	-	-	-
Super-Bainite 9	0.67	1.60	1.25	1.50	-	-	-	-	-
Super-Bainite 10	0.61	1.45	0.76	2.42	-	-	-	-	-
Super-Bainite 11	0.64	1.60	1.27	1.50	-	-	0.03	-	-
Super-Bainite 12	0.58	1.63	1.29	1.43	0.1	-	-	-	-

Table 2 Tetragonality values and carbon content in ferrite determined by X-ray diffraction (XRD) analysis of Super-Bainite formed at different temperatures and times in comparison with martensite (as-quench sample) and tempered martensite (Quenched and tempered, Q&T, sample); and corresponding atom probe tomography (APT) data measured randomly distributed and as carbon clusters in bainitic ferrite.

Steel and Heat Treatment	c/a values XRD	Carbon content in ferrite XRD, at.%	Carbon in matrix APT, at.%	Carbon in clusters APT, at.%
Fe-0.7C-1.4Si-1.4Mn-1.0Cr wt.% (*modified Super-Bainite 9*)				
Fe-3.0C-2.8Si-1.3Mn-1.1Cr at.%:				
As-quench	1.0332±0.0004	2.80±0.04	–	10.04±0.50
220ºC / 24 h.	1.0083±0.0004	0.87±0.04	0.22±0.01	10.90±0.56
220ºC / 168 h.	1.0082±0.0004	0.86±0.04	0.13±0.01	10.52±0.68
250ºC / 8 h.	1.0077±0.0004	0.81±0.04	0.14±0.01	10.92±0.31
300ºC / 5 h.	1.0071±0.0004	0.73±0.04	0.14±0.01	9.68±0.83
Fe-1.0C-1.3Si-1.0Mn-1.4Cr wt.% (*modified Super-Bainite 4*)				
Fe-4.3C-2.4Si-1.0Mn-1.4Cr at.%:				
Q&T 230ºC / 80 h.	1.0080±0.0002	0.82±0.04	0.28±0.02	11.00±0.3
230ºC / 35 h.	1.0090±0.0002	0.87±0.04	0.14±0.01	10.20±2.7
Fe-1.0C-2.9Si-0.8Mn-0.4Cr wt.% (*Super-Bainite 7*)				
Fe-4.3C-5.4Si-0.8Mn-0.4Cr at.%:				
200ºC / 40 h.	1.0090±0.0004	0.95±0.04	0.13±0.01	12.64±0.4
250ºC / 15 h.	1.0084±0.0004	0.90±0.04	0.10±0.01	12.54±0.3

Table 3. Hardness values and tensile properties of Super-Bainite (Caballero and Bhadeshia 2004, Garcia-Mateo, Caballero et al. 2012, Sourmail, Caballero et al. 2013, Caballero, Garcia-Mateo et al. 2014).

Steel	Heat Treatment	Hardness HV30	YS MPa	UTS MPa	UElong %	TElong %
First Generation:						
Super-Bainite 0	250ºC / 48h	580	2500 (*compression)*	-	-	-
Super-Bainite 1	250ºC / 72h	550	-	-	-	-
Super-Bainite 2	200ºC / 72h	660	1450	2200	5	5.0
	250ºC / 14h	589	1500	2050	14	20.0
	300ºC / 6h	500	1200	1750	-	29.0
Super-Bainite 3	200ºC / 72h	650	1710	2260	7.6	7.6
	250ºC / 12h	565	1770	1930	7	9.4
	300ºC / 6h	500	1200	1700	-	27.0
Second Generation:						
Super-Bainite 4	250ºC / 16h	652	1834	2205	3.9	11.2
Super-Bainite 5	220ºC / 22h	714	1798	-	0.9	0.9
	240ºC / 16h	691	1866	2278	4.9	7.2
Super-Bainite 6	200ºC / 64h	751	2019	2091	0.4	0.4
	220ºC / 22h	707	1883	-	0.3	0.3
	250ºC / 16h	659	1852	2164	2.9	8.3
Super-Bainite 7	220ºC / 22h	650	1704	2287	7.4	7.4
	250ºC / 16h	625	1698	2068	11.6	21.3
Super-Bainite 8	220ºC / 40h	710	1931	2329	3.2	4.1
	250ºC / 22h	659	1910	2213	3.0	11.9
	270ºC / 7h	615	1701	2036	4.4	12.6
Super-Bainite 9	250ºC / 12h	591	1484	2023	7.8	14.2
Super-Bainite 10	250ºC / 12h	589	1582	2030	7.8	14.2
Super-Bainite 11	220ºC / 22h	634	1358	2234	5.1	5.1

	250ºC / 12h	595	1480	2017	7.6	19.1
Super-Bainite 12	220ºC / 22h	602	1443	2022	7.0	19.1